the plant journal

SEB SOCIETY FOR EXPERIMENTAL BIOLOGY

The Plant Journal (2024) doi: 10.1111/tpj.16759

EpMYB2 positively regulates chicoric acid biosynthesis by activating both primary and specialized metabolic genes in purple coneflower

Ge Jin, Zongbi Deng, Hsihua Wang, Yang Zhang and Rao Fu*

Key Laboratory of Bio-Resource and Eco-Environment of Ministry of Education, College of Life Sciences, Sichuan University, Chengdu 610065, People's Republic of China

Received 7 November 2023; revised 20 March 2024; accepted 25 March 2024.
*For correspondence (e-mail rao@scu.edu.cn).

SUMMARY

Chicoric acid is the major active ingredient of the world-popular medicinal plant purple coneflower (*Echinacea purpurea* (L.) Menoch). It is recognized as the quality index of commercial hot-selling Echinacea products. While the biosynthetic pathway of chicoric acid in purple coneflower has been elucidated recently, its regulatory network remains elusive. Through co-expression and phylogenetic analysis, we found EpMYB2, a typical R2R3-type MYB transcription factor (TF) responsive to methyl jasmonate (MeJA) simulation, is a positive regulator of chicoric acid biosynthesis. In addition to directly regulating chicoric acid biosynthetic genes, EpMYB2 positively regulates genes of the upstream shikimate pathway. We also found that EpMYC2 could activate the expression of *EpMYB2* by binding to its G-box site, and the EpMYC2–EpMYB2 module is involved in the MeJA-induced chicoric acid biosynthesis. Overall, we identified an MYB TF that positively regulates the biosynthesis of chicoric acid by activating both primary and specialized metabolic genes. EpMYB2 links the gap between the JA signaling pathway and chicoric acid biosynthesis. This work opens a new direction toward engineering purple coneflower with higher medicinal qualities.

Keywords: purple coneflower, chicoric acid, biosynthesis, MYB transcription factor, co-expression, transcriptional regulation, shikimate pathway.

INTRODUCTION

For millennia, humankind has used plants for medicinal purposes to maintain our health (Fu, Li, Yu, et al., 2021). Natural product molecules are vital resources for drug development (Newman & Cragg, 2020). Purple coneflower (*Echinacea purpurea* (L.) Menoch) originates from North America and is widely cultivated worldwide. In addition to being grown as an ornamental plant, it has been used as an herbal medicine for treating mouth sores, colds, and snakebites (Kindscher, 2016). Modern pharmacology experiments have proved it has immunomodulating, anti-inflammatory, antioxidant, and antivirus activities (Burlou-Nagy et al., 2022). Echinacea products have sold well worldwide for decades (Smith et al., 2022). They are taken to prevent and treat common colds (Karsch-Volk et al., 2015; Shah et al., 2007). Many different chemical components have been identified in purple coneflower, including caffeic acid derivatives, glycoproteins, alkylamines, and flavonoids (Kindscher, 2016). Chicoric acid, a caffeic acid derivative, is the most representative of these diverse chemicals and accumulates in whole plants. It has been used as a quality index for Echinacea products and raw purple coneflower materials. Many reports have demonstrated that chicoric acid possesses various bioactivities, such as antivirus, antioxidant, anti-inflammation, liver protection, kidney protection, and anticancer, which have been reviewed recently (Yang et al., 2022). So far, purple coneflower has been the major resource of chicoric acid supplements (Yang et al., 2022). Due to the high market requirement of purple coneflower and chicoric acid, it is necessary to increase the chicoric acid content in planta, which is depending on the elucidation of the biosynthetic pathway and regulatory network (Isah et al., 2018).

Previously, we have elucidated the biosynthetic pathway of chicoric acid in purple coneflower (Fu, Zhang, Jin, et al., 2021). First, the phenylalanine is converted to *p*-coumaroyl CoA by the rate-limiting enzyme phenylalanine ammonia-lyase (PAL) and the following cinnamate 4-hydroxylase (C4H) and 4-coumarate: CoA ligase (4CL). *p*-Coumaroyl CoA is the crucial intermediate for the biosynthesis of diverse phenylpropanoids, including flavonoids, hydroxycinnamic acid derivatives, and stilbenes (Vogt, 2010).

For chicoric acid biosynthesis, *p*-coumaroyl CoA is converted to caffeoyl CoA by hydroxycinnamoyl-CoA: shikimate/quinate hydroxycinnamoyl transferase (HCT) and *p*-coumaroyl shikimic/quinic acid 3′-hydroxylase (C3′H). Two BAHD-type acyltransferases, hydroxycinnamoyl-CoA: tartaric acid hydroxycinnamoyl transferase (HTT) and hydroxycinnamoyl-CoA: quinate hydroxycinnamoyl transferase (HQT), utilize caffeoyl CoA as the acyl donor to produce caftaric acid and chlorogenic acid using tartaric acid and quinic acid as acyl acceptor, respectively. Finally, a special serine carboxypeptidase-like (SCPL) type acyltransferase, chicoric acid synthase (CAS), catalyzes the biosynthesis of chicoric acid using caftaric acid as the acyl acceptor and chlorogenic acid as the acyl donor (Figure 1A) (Fu, Zhang, Jin, et al., 2021). We further described the substrate promiscuity of acyltransferase and depicted the whole biosynthesis network of chicoric acid and its analogs in purple coneflower (Fu et al., 2022). Undoubtedly, chicoric acid accumulation is determined by the expression of its biosynthetic genes (Fu, Zhang, Deng, et al., 2021; Fu, Zhang, Jin, et al., 2021; Xiang et al., 2022). Meanwhile, the expression of biosynthetic genes is usually regulated by transcription factors (TFs) (Deng & Lu, 2017; Liu et al., 2015; Zheng et al., 2023). Although we have elucidated the biosynthetic pathways, the regulatory network of chicoric acid remains unclear.

Plant TFs from various families have been identified to regulate plant secondary metabolism, such as *v-Myb* myeloblastosis viral oncogene homolog (MYB), basic/helix–loop–helix (bHLH), WD-repeat, ethylene-responsive factor (ERF), WRKY, and basic leucine zipper (bZIP) (Dong & Lin, 2021; Yang et al., 2012). Among them, MYB TFs are reported to be the major regulators of phenylpropanoid

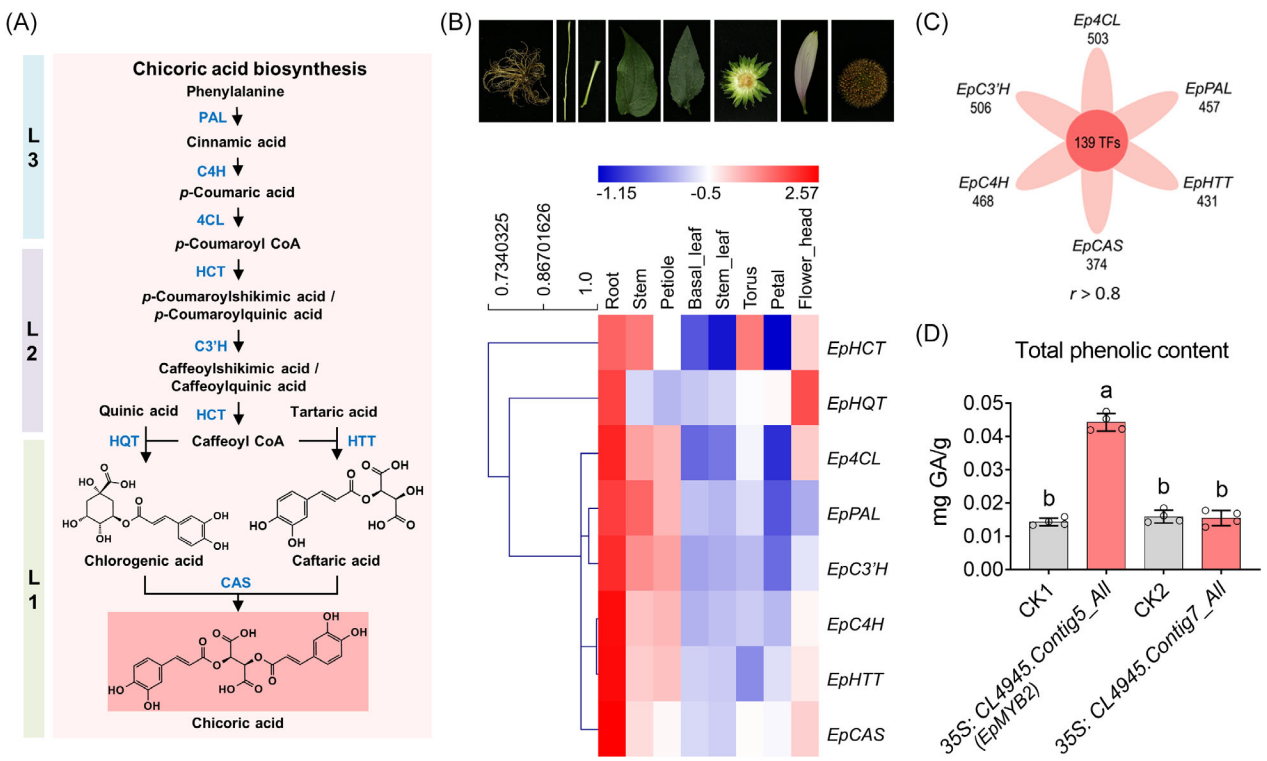

Figure 1. Candidate chicoric acid biosynthesis regulator is identified by co-expression.
(A) The biosynthetic pathway of chicoric acid. The chicoric acid biosynthetic pathway is divided into three levels: level 1 (L1) is the chicoric acid-specific pathway from caffeoyl CoA to chicoric acid, level 2 (L2) is from *p*-coumaroyl CoA to caffeoyl CoA, sharing with other hydroxycinnamic acid derivatives, and level 3 (L3) is the common phenylpropanoid metabolic pathway from phenylalanine to *p*-coumaroyl CoA, sharing with other phenylpropanoids.
(B) Hierarchical clustering of chicoric acid biosynthetic genes. The different tissues of flowering purple coneflower are shown on the upper side. The gene per row is *Z*-score standardized and hierarchical clustered using MeV software. The tightly co-expressed structure genes pave the way for the use of co-expression analysis for the screening of candidate regulators.
(C) A total of 139 TFs are obtained from the intersection of co-expressed genes with six structural genes. Co-expression analysis ($r > 0.8$) using *EpPAL*, *EpC4H*, *Ep4CL*, *EpC3′H*, *EpHTT*, and *EpCAS* as baits is performed using Microsoft EXCEL CORREL function to screen chicoric acid biosynthesis regulators.
(D) Transient over-expression of candidate *EpMYBs* in *N. benthamiana* leaves results in changes in the total phenolic content. Phylogenetic analysis (Figure S2B) is performed to narrow candidates. Furthermore, according to the functional classification of MYB subfamilies, these two EpMYBs belonging to subfamily 7 are selected for functional verification. Lower cases indicate a significant difference ($P < 0.05$) among groups. Data are shown as mean ± SD ($n = 4$). PAL, phenylalanine ammonia-lyase; C4H, cinnamate 4-hydroxylase; 4CL, 4-coumarate: CoA ligase; HCT, hydroxycinnamoyl-CoA: shikimate/quinate hydroxycinnamoyl transferase; C3′H, 4-coumaroyl shikimic/quinic acid 3′-hydroxylase; HQT, hydroxycinnamoyl-CoA: quinate hydroxycinnamoyl transferase; HTT, hydroxycinnamoyl-CoA: tartaric acid hydroxycinnamoyl transferase; CAS, chicoric acid synthase.

metabolism (Liu et al., 2015). They comprise a conserved N-terminal DNA-binding domain repeat (R) and a variable C-terminal regulatory region. The R can be classified into R1, R2, and R3 based on sequence similarity. Based on the number of R, MYBs can be divided into four classes, including 1R-, R2R3-, 3R-, and 4R-MYB proteins (Jiang & Rao, 2020). The R2R3-MYBs, which predominate in plant MYBs, are thought to have helped plants adapt from aquatic to terrestrial environments with functional diversification (Jiang & Rao, 2020; Wu et al., 2022). R2R3-MYBs from subfamilies 3, 4, 5, 6, 7, 8, 13, 21, 31, 32, 44, and 79 are mainly reported to regulate the phenylpropanoid biosynthetic pathway as activators or repressors by directly binding to the promoters (Wu et al., 2022). Many plant R2R3-MYBs recognize AC elements of the DNA target, which are enriched in adenosine and cytosine residues (Prouse & Campbell, 2012). For example, AtMYB12, a subfamily 7 member, has been reported to directly bind to MYB12BS sites (CACCTACC, TACCTAMC, and TAGCWACC) on promoters of *enolase* (*ENO*), *3-deoxy-D-arabinoheptulosonate 7-phosphate synthase* (*DAHPS*), *PAL*, *chalcone synthase* (*CHS*), and *flavanone 3-hydroxylase* (*F3H*) (Zhang et al., 2015).

Furthermore, biotic and abiotic simulation also affect the biosynthesis of plant secondary metabolites (Erb & Kliebenstein, 2020). Induced plant defense is associated with producing a vast array of secondary metabolites (Guo et al., 2018). During this process, jasmonates (JAs), the lipid-derived plant hormones, play a critical role (De Geyter et al., 2012). For example, JAs induce the biosynthesis of many secondary metabolites, such as vinblastine, artemisinin, nicotine, and paclitaxel (Afrin et al., 2015). Many TF families, including MYB, ERF, bHLH, and WRKY, whose members are JAs-responsive and regulate the JAs-induced secondary metabolite accumulation (Zhou & Memelink, 2016). In the JA signaling pathway, the JA ZIM domain (JAZ) family of repressor proteins usually binds to TFs and inhibits their activation functions. In the presence of JAs, JAZ proteins are degraded by the SCF^{COI1} complex, ultimately releasing TFs. The best-studied TFs in this pathway belong to the MYC family (bHLH type TF), including MYC2, MYC3, and MYC4. For example, MYC2s, directly and indirectly, regulate secondary metabolite induction (Song et al., 2022), which binds to the G-box sites on the promoters of downstream genes and activates their expression (Zhai et al., 2020).

Interestingly, the biosynthesis of chicoric acid in purple coneflower hairy roots, seedlings, and cell suspension cultures is significantly induced by methyl jasmonate (MeJA) (Fu, Zhang, Jin, et al., 2021; Ravazzolo et al., 2022; Tahmasebi et al., 2019). Which kind of TFs are involved in the MeJA-induced chicoric acid biosynthesis in purple coneflower remains elusive. Combining TFs and biosynthetic genes will significantly increase the target metabolite yield (Zhang et al., 2015). Therefore, potential positive regulators must be identified for high chicoric acid production. Recently, we have established a multi-tissue transcriptome of flowering purple coneflower and identified an R2R3-MYB TF, EpMYB1, belonging to the subfamily 6, positively regulates anthocyanin biosynthesis in purple coneflower (Jin et al., 2024). Here, based on this multi-tissue transcriptome, we used co-expression and phylogenetic analysis to identify potential TFs involved in chicoric acid biosynthesis. Through systemic characterization and *in vivo* transgenic verification, an MYB TF was identified, and its regulatory mechanism was elucidated. Further investigation also explained its role in MeJA-induced chicoric acid biosynthesis. This study further explains chicoric acid biosynthesis and paves the way for applying biotechnological approaches to increase chicoric acid contents in purple coneflower.

RESULTS

Screening of TFs involved in chicoric acid biosynthesis

Previously, we have elucidated the biosynthetic pathway of chicoric acid in purple coneflower (Figure 1A) (Fu, Zhang, Jin, et al., 2021). Using the recently established multi-tissue transcriptome (Jin et al., 2024), the chicoric acid biosynthetic genes were identified using the BLASTP method (Table S1). After hierarchical clustering analysis of the expression levels of these biosynthetic genes, we found similar expression patterns, and they were all highly expressed in roots (Figure 1B). *EpPAL*, *EpC4H*, *Ep4CL*, *EpC3′H*, *EpHTT*, and *EpCAS* were especially tightly co-expressed (Figure 1B). These results were verified using RT-qPCR (Figure S1).

Co-expression analysis among metabolites, structural genes, and TFs has been widely used for the identification of intermediate substrates, biosynthetic genes, and regulators (Fu et al., 2022; Hong et al., 2022; Jin et al., 2024; Li et al., 2020; Reed et al., 2023; Ren et al., 2022; Yuan et al., 2022). We then used the six highly correlated chicoric acid biosynthetic genes as baits for co-expression analysis. A total of 139 TFs were obtained from the intersection of the six biosynthetic genes' correlated genes with a linear coefficient above 0.8 (Figure 1C). MYB TFs have been demonstrated to regulate phenylpropanoid metabolism (Liu et al., 2015; Zheng et al., 2023). Among the 139 TFs, 21 were annotated as MYB (Figure S2A and Supplemental Data Set S1). After removing the redundant sequences, 10 of the 21 EpMYBs were aligned with AtMYBs and used for phylogenetic analysis (Figure S2B). These EpMYBs were distributed in several subfamilies, including 2, 7, 14, 20, and 78. Previously, members of subfamilies 3, 4, 5, 6, 7, 8, 13, 21, 31, 32, 44, and 79 have been reported to be involved in regulating phenylpropanoid biosynthesis (Wu et al., 2022). Among the ten EpMYBs, there were two

subfamily 7 members, namely CL4945.Contig5_All and CL4945.Contig7_All, might have potential phenylpropanoids regulating functions. When these two EpMYBs were transiently overexpressed in *Nicotiana benthamiana* leaves, CL4945.Contig5_All (named EpMYB2) significantly increased the total phenolic content (Figure 1D). Overall, we identified EpMYB2 as the potential chicoric acid biosynthesis regulator through co-expression, phylogenetic analysis, and heterologous functional research.

EpMYB2 positively regulates chicoric acid biosynthesis

Multiple sequence analysis of EpMYB2 with members of the subfamily 7 in *Arabidopsis thaliana* revealed that EpMYB2 has complete R2 and R3 domains, identifying it as an R2R3-MYB (Figure S3). Further phylogenetic analysis of EpMYB2 with subfamily 7 members from other plant species indicated that EpMYB2 was close to GtMYBP4 from *Gentiana trifloral*, which has been reported to promote flavonol biosynthesis (Figure 2A) (Nakatsuka et al., 2012). The RT-qPCR analysis showed that *EpMYB2* was highly expressed in roots, stems, and petioles, consistent with RNA-seq data (Figure 2B). Through transient expression of EpMYB2-GFP fusion protein in tobacco leaves, EpMYB2 was found nuclear localized (Figure 2C). In addition, the expression of *EpMYB2* responded to different stress treatments, especially MeJA (Figure 2D), suggesting its potential role in linking environmental stress and secondary metabolism (Fu, Zhang, Jin, et al., 2021; Tahmasebi et al., 2019).

To explore the *in vivo* function of EpMYB2, we constructed *EpMYB2*-OE purple coneflower calli (Figure S4). The phenotypes of CK and *EpMYB2*-OE calli were both faint yellow and showed no significant difference from each other (Figure 3A). The *EpMYB2* expression level of the *EpMYB2*-OE group was significantly higher than that of the CK group ($P < 0.05$) (Figure 3B). A non-target metabolomic approach based on LC-HRMS with three biological pools of purple coneflower calli was adopted to evaluate the metabolite change induced by *EpMYB2*-OE (Fu, Zhang, Deng, et al., 2021). From the principal component analysis (PCA) score plot, the CK group and the *EpMYB2*-OE group were significantly separated (Figure 3C). Further evaluation of the loading plot demonstrated that the major differential ions belong to chicoric acid, its analogs methylchicoric acid, and its substrates caftaric acid and chlorogenic acid, identified based on retention times and mass spectrum according to

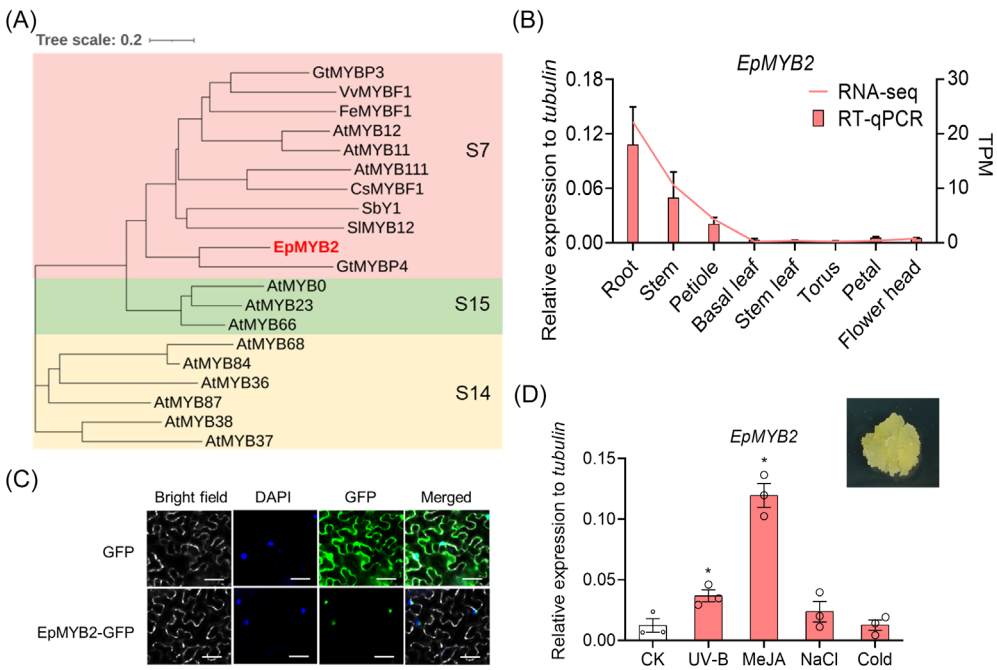

Figure 2. EpMYB2 is a MeJA-responsive nuclear localized MYB.
(A) Phylogenetic analysis shows that EpMYB2 is a member of MYB subfamily 7. The other functional characterized MYBs for phylogenetic analysis including AtMYB12 (O22264), SlMYB12 (NP_001234401), AtMYB11 (Q9LZK4), AtMYB111 (Q9FJ07), FeMYBF1 (BBC70848), GtMYBP3 (BAM71801), GtMYBP4 (BAF96934), SbY1 (AAX44239), VvMYBF1 (NP_001267930), CsMYBF1 (AMH40451), AtMYB36 (Q9FKL2), AtMYB37 (Q9FG68), AtMYB38 (Q9SJL7), AtMYB68 (NP_201380), AtMYB84 (Q9M2Y9), AtMYB87 (F4JSU0), AtMYB0 (P27900), AtMYB23 (Q96276), AtMYB66 (Q9SEI0).
(B) *EpMYB2* is highly expressed in roots determined by RT-qPCR. *Eptubulin* is used as the reference gene. Data are shown as mean ± SD ($n = 3$).
(C) EpMYB2 is a nuclear-localized protein in *N. benthamiana* leaves. DAPI is used as a nuclear marker. Scale bars, 50 μm.
(D) EpMYB2 is a MeJA-responsive MYB TF. The expression level of *EpMYB2* in purple coneflower calli treated with different environmental stresses for 6 h is determined by RT–qPCR. * indicates the significant difference ($P < 0.05$) compared to CK. Data are shown as mean ± SD ($n = 3$).

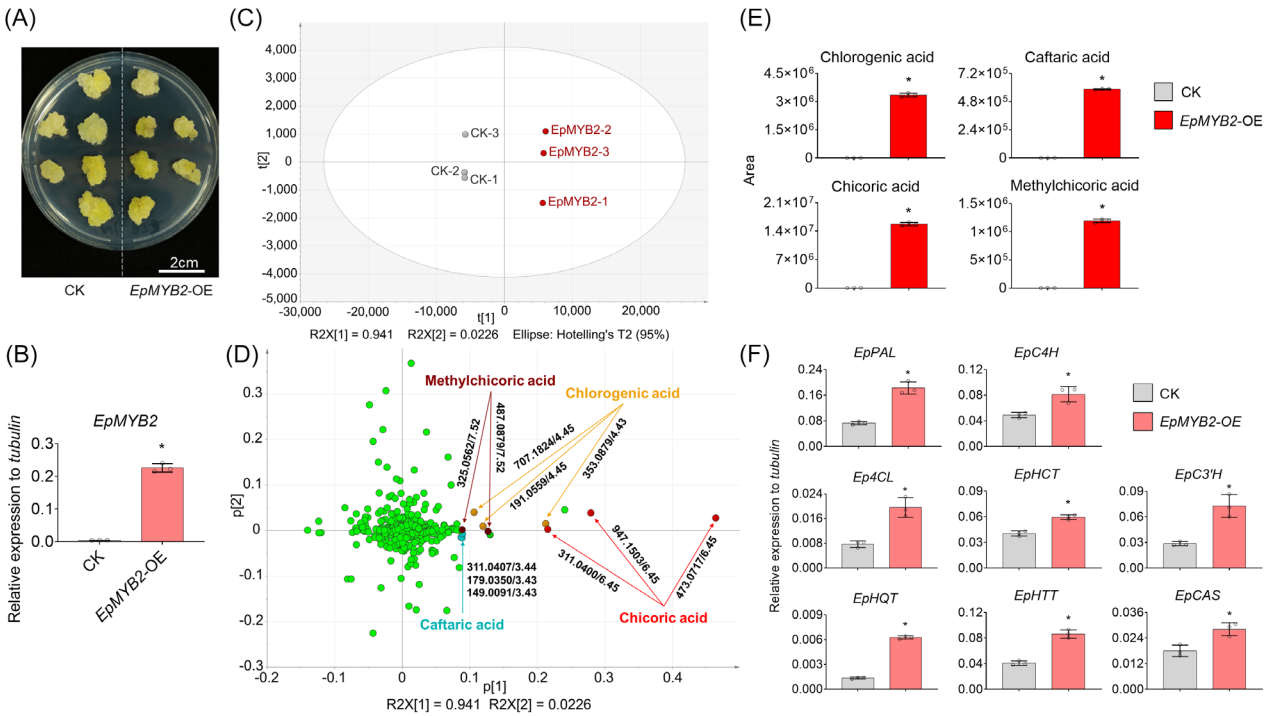

Figure 3. EpMYB2 positively regulates the biosynthesis of chicoric acid in purple coneflower calli.
(A) The similar phenotypes of control check (CK) and *EpMYB2*-OE calli lines. *EpMYB2* is over-expressed in purple coneflower calli to investigate its *in vivo* role.
(B) *EpMYB2* is significantly over-expressed compared to CK determined by RT-qPCR.
(C) *EpMYB2*-OE changes the metabolism of purple coneflower calli. A non-targeted metabolomics approach is used to evaluate the effects of *EpMYB2*-OE on the metabolism. CK and *EpMYB2*-OE groups are separated in the PCA scoring plot, suggesting different metabolomics.
(D) Chicoric acid and its analog and substrates are the major different compounds between CK and *EpMYB2*-OE presented by the loading plot of PCA analysis. These ions are identified by comparing the retention time and the mass spectrum between samples and reference standards or previously identified compounds.
(E) The level of chicoric acid and its analog and substrates are significantly increased by *EpMYB2*-OE determined by LC-HRMS analysis. *EpMYB2* shows a positive regulatory effect on the biosynthesis of chicoric acid.
(F) The expression levels of chicoric acid biosynthetic genes are induced by *EpMYB2*-OE determined by RT–qPCR. The upregulated biosynthetic genes result in the accumulation of metabolites. * indicates the significant difference ($P < 0.05$) compared to CK. Data are expressed as mean ± SD ($n = 3$).

the previous report (Figure 3D) (Fu et al., 2022). Compared to the CK group, the levels of these chemicals in the *EpMYB2*-OE group were significantly increased (Figure 3E). Besides, the chicoric acid biosynthetic genes, including *EpPAL*, *EpC4H*, *Ep4CL*, *EpHCT*, *EpC3'H*, *EpHQT*, *EpHTT*, and *EpCAS*, were all upregulated by EpMYB2 (Figure 3F). These results demonstrated that EpMYB2 is a positive regulator of chicoric acid biosynthesis. On the other side, as members from the subfamily 7 have been identified to be flavonoid regulators (Liu et al., 2015; Wu et al., 2022), we further investigated the effect of EpMYB2 on flavonoids. EpMYB2 did not show consistent facilitation to key biosynthetic genes' expression and representative chemicals' levels of flavonoids (Figure S5). It significantly increased the level of rutin but not that of nicotiflorin. The increase in chicoric acid was much higher than that of rutin, suggesting that the activation of chicoric acid biosynthesis by EpMYB2 is more robust than that of flavonoids. All these results demonstrated that EpMYB2 mainly promotes chicoric acid biosynthesis in purple coneflower.

EpMYB2 positively regulates upstream primary metabolic genes

Many TFs have been found to have multiple regulatory targets, especially some TFs regulating secondary metabolism, which have been identified to be involved in the regulation of primary metabolism (Zhang et al., 2015). To further evaluate the function of EpMYB2, we performed RNA-seq analysis of transgenic calli (Figure S6). The upregulated genes were put into the KEGG pathway enrichment analysis. Interestingly, in addition to the phenylalanine metabolism, the phenylalanine, tyrosine, and tryptophan biosynthesis pathway was enriched (Figure 4A). These aromatic amino acids are derived from the shikimate pathway, which belongs to primary metabolism, and is the upstream of phenylpropanoid metabolism (Vogt, 2010). We identified these upstream biosynthetic genes by BLASTP using homologs from other plant species (Figure 4B; Table S1) and evaluated their expression levels using RT-qPCR. Several structural genes, including

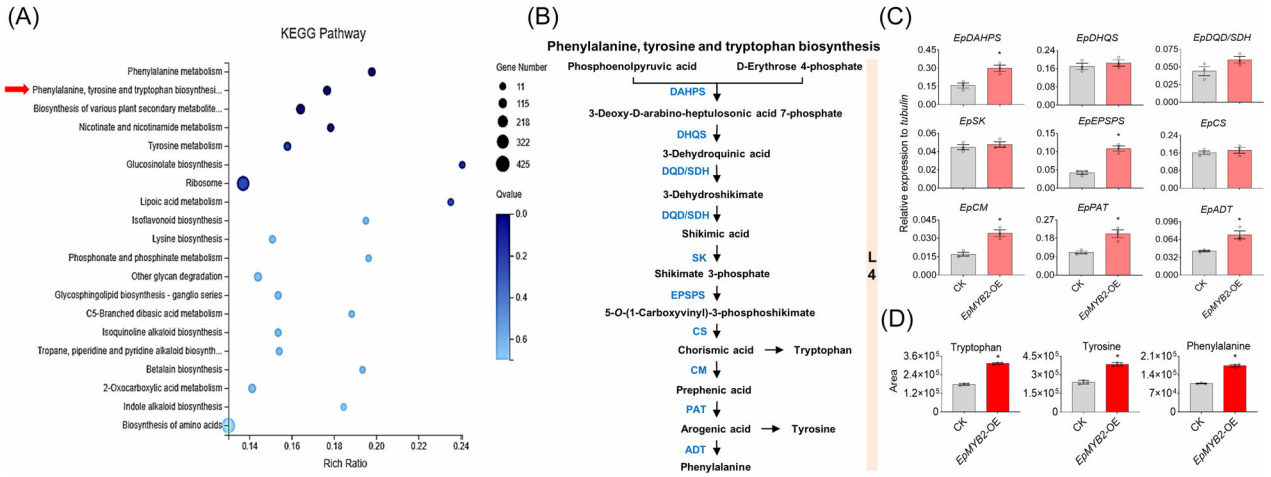

Figure 4. EpMYB2 promotes the biosynthesis of aromatic amino acids.
(A) In addition to the phenylalanine metabolism, the up-regulated genes by EpMYB2 are enriched to phenylalanine, tyrosine, and tryptophan biosynthesis pathways. RNA-seq analysis of transgenic calli is performed to further evaluate the *in vivo* function of *EpMYB2*. The differently expressed genes are analyzed by KEGG pathway enrichment analysis. The size and color of the dot represent the gene number and Q value, respectively.
(B) The phenylalanine, tyrosine, and tryptophan biosynthetic pathway. From the shikimate pathway to aromatic amino acids, generation is assumed as the level 4 (L4) for chicoric acid biosynthesis.
(C) EpMYB2 significantly induces the expression of several structure genes of the L4 pathway determined by RT-qPCR.
(D) The levels of phenylalanine, tyrosine, and tryptophan are significantly increased by EpMYB2 determined by LC–HRMS analysis. In c and d, * indicates the significant difference ($P < 0.05$) compared to CK. Data are shown as mean ± SD ($n = 3$). DAHPS, 3-deoxy-D-arabino-heptulosonate 7-phosphate synthase; DHQS, 3-dehydroquinate synthase; DQD/SDH, 3-dehydroquinate dehydratase/shikimate 5-dehydrogenase; SK, shikimate kinase; EPSPS, 3-phosphoshikimate 1-carboxyvinyltransferase; CS, chorismate synthase; CM, chorismate mutase; PAT, prephenate aminotransferase; ADT, arogenate dehydratase.

EpDAHPS, *EpEPSPS*, *EpCM*, *EpPAT*, and *EpADT*, were significantly upregulated by EpMYB2 ($P < 0.05$) (Figure 4C). Consequently, the levels of tryptophan, tyrosine, and phenylalanine were all significantly increased ($P < 0.05$) (Figure 4D). In summary, EpMYB2 was found to have multiple potential regulatory targets covering primary and secondary metabolic pathways.

EpMYB2 activates the expression of key phenylalanine and chicoric acid biosynthetic genes through direct binding

To explore the regulatory mechanism of EpMYB2 on the biosynthesis of chicoric acid, we tried to clone the promoters of these primary and secondary metabolic genes. Ten promoters were successfully cloned using the previously reported method (Figure 5B) (Tan et al., 2019). We then adopted a dual-luciferase assay to test the activation of EpMYB2 on these promoters (Figure 5A). EpMYB2 showed activation effects on *proEpCM*, *proEpPAT*, *proEpPAL*, *proEpC4H*, *proEp4CL*, *proEpHCT*, *proEpC3'H*, *proEpHTT*, and *proEpCAS*, but not *proEpHQT* (Figure 5C). The key metabolic genes leading the flux to chicoric acid biosynthesis, *EpPAL*, *EpHCT*, and *EpHTT*, were extensively activated (Figure 5C). *EpHQT* has also shown distinct expression patterns in the seed germination process of purple coneflower, suggesting its different regulation network (Xiang et al., 2022). These results demonstrated that EpMYB2 can directly activate the promoters of important metabolic genes and result in the biosynthesis of chicoric acid. To further identify the potential binding sites, we analyzed these promoters and found that *proEpCM*, *proEpPAT*, *proEpPAL*, *proEpHCT*, *proEpC3'H*, and *proEpHTT* all contain MYB12BS sites within 500 bp of the upstream of ATG (Figure 5B). We selected *EpPAL*, *EpHCT*, and *EpHTT*, the key metabolic genes for chicoric acid biosynthesis, to investigate the potential binding site. Mutation of the MYB12BS site on *proEpPAL*, *proEpHCT*, and *proEpHTT* significantly decreased the activation level of EpMYB2 on these promoters in the dual-luciferase assay (Figure S7A; Figure 5D,F). Furthermore, we adopted a yeast one-hybrid (Y1H) assay to confirm the direct binding effects. EpMYB2 showed direct binding to *proEpHCT* and *proEpHTT* at MYB12BS sites (Figure 5E,G). Due to the high auto-activity of *proEpPAL*, it was hard to verify the direct binding effect of EpMYB2 on it (Figure S7B). These results indicated that the MYB12BS is at least one of the binding sites of EpMYB2. In summary, we found that EpMYB2 can directly activate gene expression by binding to promoters and identifying a binding site.

The EpMYC2-EpMYB2 module mediates the MeJA-induced chicoric acid biosynthesis

Previous reports showed that the chicoric acid biosynthesis in purple coneflower is induced by MeJA (Fu, Zhang, Jin, et al., 2021; Ravazzolo et al., 2022; Tahmasebi et al., 2019). In this study, we noticed that the expression of *EpMYB2*

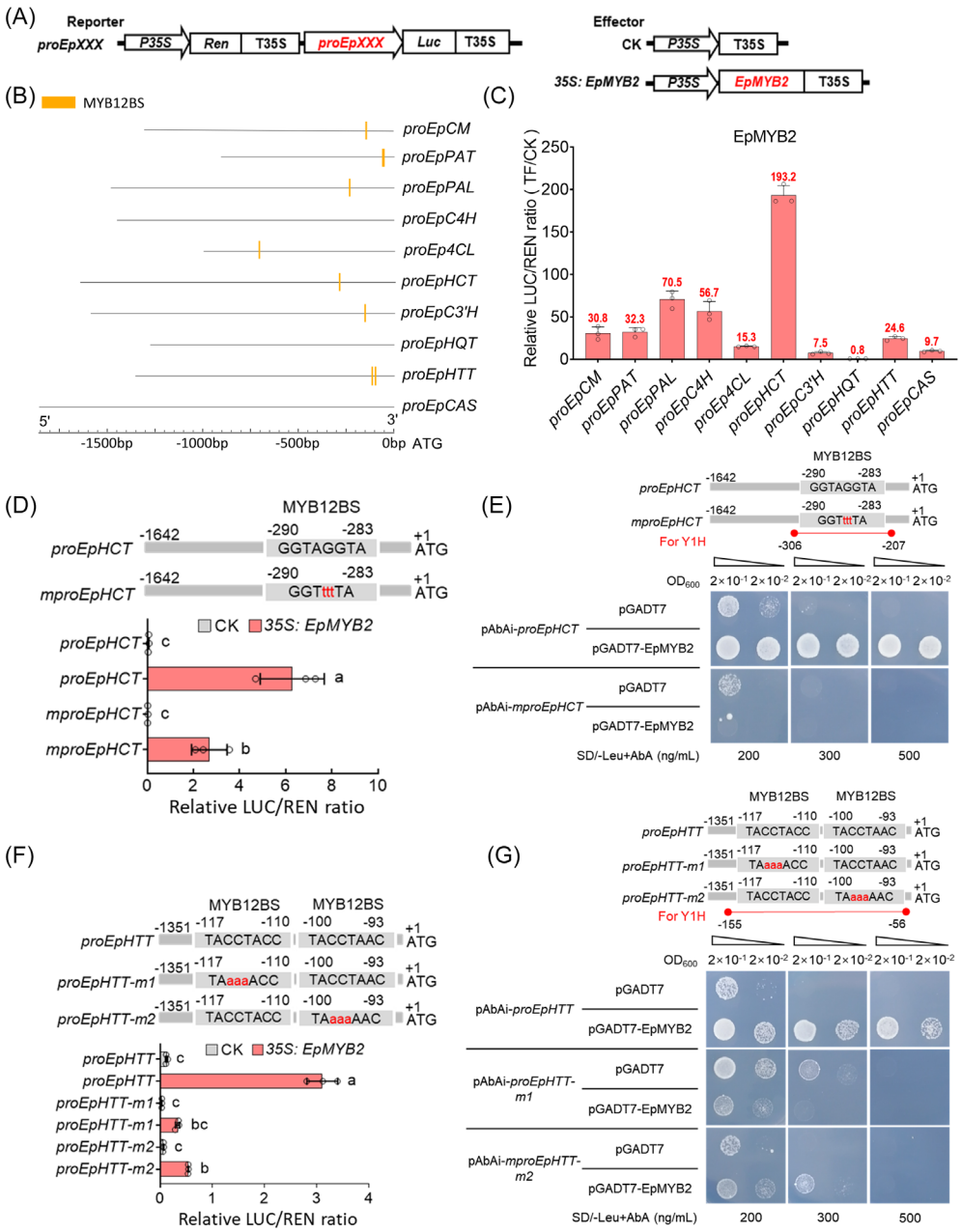

Figure 5. EpMYB2 activates the expression of both primary and specialized biosynthetic genes.
(A) Schematic diagrams of vectors used for the dual-luciferase assay to investigate the regulatory mechanism of EpMYB2 on the biosynthesis of chicoric acid.
(B) Successful cloned promoters of biosynthetic genes. Potential binding site MYB12BS (AtMYB12 binding site, CACCTACC, TACCTAMC, and TAGCWACC) is distributed on promoters.
(C) EpMYB2 activates different promoters of metabolic genes determined by dual-luciferase assay. Data are expressed as the ratio of EpMYB2 and CK. Data are shown as mean ± SD (n = 3). To further identify the potential binding sites, dual-luciferase assay and Y1H assays are adopted. EpMYB2 directly binds to *proEpHCT* at MYB12BS, determined by dual-luciferase assay (D) and Y1H (E). EpMYB2 also directly binds to the two MYB12S sites of *proEpHTT* verified by dual-luciferase assay (F) and Y1H (G). After mutation, the activation effects significantly decrease, implying the importance of MYB12S sites. Lower cases in D and F indicate a significant difference ($P < 0.05$) among groups. Data are shown as mean ± SD (n = 3).

was significantly influenced by MeJA (Figure 2D), which led us to wonder if EpMYB2 was involved in the MeJA-induced chicoric acid biosynthesis. As *EpMYB2* is mainly expressed in roots (Figure 2), we treated purple coneflower roots with MeJA to further explore the role of EpMYB2 in responding to the JA signaling. The expression level of *EpMYB2* was significantly increased by MeJA treatment (Figure 6A). Furthermore, the chicoric acid biosynthetic gene expression levels and chemical contents were all induced (Figure 6B). As the important role of MYC2 in

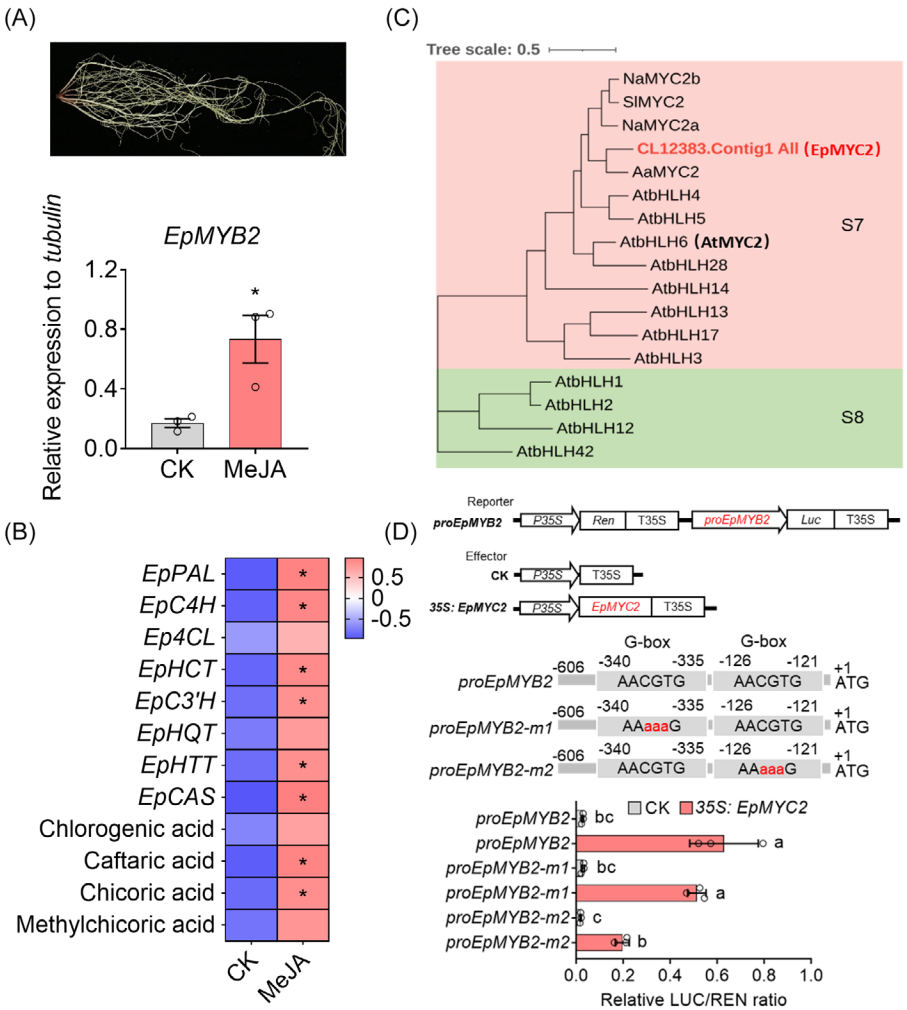

Figure 6. The EpMYC2-EpMYB2 module mediates the MeJA-induced chicoric acid biosynthesis.
(A) *EpMYB2* of purple coneflower root is induced by MeJA treatment determined by RT–qPCR. As chicoric acid biosynthetic genes are mainly expressed in roots, MeJA is applied to roots to study EpMYB2's role in the JA signaling pathway.
(B) The expression levels of chicoric acid biosynthetic genes and chemical contents are significantly increased by MeJA treatment. The chemical contents are determined using LC–HRMS and the gene expression levels are measured by RT–qPCR. Data are *Z*-score standardized. * indicates the significant difference ($P < 0.05$) compared to CK.
(C) Phylogenetic analysis shows that EpMYC2 is a member of bHLH subfamily 7 (red) that includes MYC2s from other species, NaMYC2a (LOC109232914), NaMYC2b (LOC109205493), SlMYC2 (A0A3Q7HRZ6), and AaMYC2 (AKO62850). As MYC2 is a master regulator in the JA signaling pathway, the EpMYC2 is identified using BLASTP.
(D) EpMYC2 activates the *EpMYB2* promoter via the G-box site determined by dual-luciferase assay. The transcriptional activation effect of EpMYC2 on *EpMYB2* is confirmed. Lower cases indicate a significant difference ($P < 0.05$) among groups. Data are shown as mean ± SD ($n = 3$).

the JA signaling pathway (Song et al., 2022; Zhai et al., 2020), the EpMYC2 was identified by BLASTP using AaMYC2 from *Artemisia annua*, a purple coneflower closely related species (Table S1) (Shen et al., 2016). Multiple sequence alignment revealed that EpMYC2 has the complete MYC2 domains, including the basic and HLH (helix–loop–helix) domains, as well as the JAZ-interacting domain (JID) for JAZ protein binding and the transcriptional activation domain (TAD) for MED25 protein binding (Liu et al., 2019) (Figure S8). Phylogenetic analysis revealed that EpMYC2 is close to the AaMYC2 and is a typical member of the bHLH subfamily 7 (Figure 6C). To explore whether EpMYC2 could affect the expression of *EpMYB2*, the promoter of *EpMYB2* containing two G-box sites was cloned. EpMYC2 activated the promoter of *EpMYB2, which was* determined by a dual-luciferase assay (Figure 6D). The two G-box sites on the promoter were mutated separately, and when the G-box 126 bp before the ATG was mutated, the level of EpMYC2 activation on the *EpMYB2* promoter was significantly decreased (Figure 6D). The direct binding of EpMYC2 to *proEpMYB2* −126 bp G-box site was confirmed by the Y1H assay (Figure S9). Thus,

EpMYC2 activates *EpMYB2* promoter expression via the G-box site. These results indicated that the EpMYC2-EpMYB2 module mediates the MeJA-induced chicoric acid biosynthesis.

DISCUSSION

The biosynthesis of plant secondary metabolites is determined by the biosynthetic genes' expression levels, which are regulated by TFs (Zheng et al., 2023). As the major resource of chicoric acid, different strategies have been adopted to increase the chicoric acid content in purple coneflower materials (Liu et al., 2006; Ramezannezhad et al., 2019; Tabar et al., 2019). However, the underlying mechanisms remain elusive. The biosynthetic pathway and the critical regulator should be clarified to satisfy the demand for purple coneflower with high chicoric acid content (Zhou & Memelink, 2016). Previously, we have elucidated the biosynthesis pathway of chicoric acid in purple coneflower (Fu, Zhang, Jin, et al., 2021). So here, we aimed to identify the key TF that regulates the biosynthesis of chicoric acid. Many approaches have been widely used to screen TFs, such as genome-wide association study (GWAS) (Lou et al., 2022), Y1H system (Pyvovarenko & Lopato, 2011), and co-expression analysis (Li et al., 2020). Among them, co-expression analysis allows the simultaneous identification, clustering, and exploration of thousands of genes with similar expression patterns across multiple conditions. It has been widely used for the identification of intermediate substrates, biosynthetic genes, and regulators (Fu et al., 2022; Hong et al., 2022; Li et al., 2020; Reed et al., 2023; Yuan et al., 2022). The potential drawback of co-expression screening is that it usually provides many candidates (Serin et al., 2016). Phylogenetic analysis based on the sequence identity is a suitable method to narrow the number of candidates as the potential conservation of homolog gene function across different plant lineages (Ren et al., 2022; Shen et al., 2016; Yuan et al., 2022). In the present study, chicoric acid biosynthetic genes showed similar expression patterns and were used as baits for the co-expression analysis. Due to the important role of MYB TFs in regulating phenylpropanoid metabolism (Liu et al., 2015; Zheng et al., 2023), we focused on the screening of MYB TFs. Using phylogenetic analysis, we found that these EpMYBs were distributed in different subfamilies. We obtained two candidates from subfamily 7, whose members are reported to be involved in regulating phenylpropanoid metabolism (Wu et al., 2022). Through further functional verification, we identified an R2R3-MYB TF, EpMYB2, that positively regulates chicoric acid biosynthesis.

EpMYB2 is a typical R2R3-MYB TF belonging to the subfamily 7. MYBs of the subfamily 7 have previously been reported to regulate flavonoid accumulation (Liu et al., 2015). For example, FeMYBF1 from buckwheat directly activates *FeCHS*, *FeFLS*, and *FeFLS1* to induce flavonol synthesis (Matsui et al., 2018). GtMYB3 and GtMYB4 bind to promoters of *GtCHS*, *GtF3′5′H*, *GtFNSII*, and *GtF3′H* and promote the biosynthesis of flavonoid biosynthesis in *Gentiana trifloral* (Nakatsuka et al., 2012). VvMYBF1 is a specific regulator of flavonol synthesis that regulates *VvCHS*, *VvCHI*, and *VvFLS1* in grapevine (Czemmel et al., 2009). AtMYB12 activates *AtCHS*, *AtCHI*, *AtF3H*, and flavonol synthase (*FLS*) to regulate flavonoid biosynthesis in *A. thaliana* (Wang et al., 2016). In addition to regulating flavonoid biosynthesis, AtMYB12 also positively promotes the biosynthesis of caffeoylquinic acid (Luo et al., 2008). Its homolog, AtMYB11, has a greater effect on caffeoylquinic acids than AtMYB12 (Li et al., 2015). Interestingly, EpMYB2 showed a robust activation in chicoric acid biosynthesis rather than the biosynthesis of flavonoids. EpMYB2 activates the downstream specific chicoric acid biosynthetic genes and the upstream metabolic genes, including the primary metabolism pathways (Figure 7). This is similar to AtMYB12, which induces multiple primary and secondary metabolic genes, including *DAHPS*, *ENO*, *PAL*, *CHS*, and *F3H* (Zhang et al., 2015). Although the metabolic pathway target might differ, the binding sites seem quite conserved among members from subfamily 7. EpMYB2 binds to the MYB12BS sites as AtMYB12 which are similar to the MYBPLANT *cis*-element (A/C)ACC(A/T)A(A/C)C targeted by CsMYBF1 (Liu et al., 2016), and the (G/A)(G/T)T(A/T)G(G/T)T distributing in the promoters of *AtCHS*, *AtF3H*, and *AtFLS1* targeted by AtMYB111 (Li et al., 2019; Zhang et al., 2015). These results demonstrate that EpMYB2 conserves binding sites as other subfamily 7 members but adjusts the major regulatory targets. These results also suggest the potential regulatory effects of other subfamily 7 members on the other branch rather than flavonoids in phenylpropanoid metabolism.

Plant secondary metabolites play critical roles in plant-environment interactions. They are synthesized by corresponding biosynthetic enzymes in different organs or tissues at particular developmental stages and respond to various environmental stimuli (Yang et al., 2012). In this process, multiple TFs integrate internal and external signals to regulate the expression of biosynthetic genes (Yang et al., 2012). Some of them are JA-responsive (Zhou & Memelink, 2016). When plants are mechanically damaged or eaten by insects, they can induce the production of JA, which triggers the JA signaling pathway (Creelman et al., 1992). Previous reports have proved that chicoric acid biosynthesis is induced by MeJA in purple coneflower different materials including hairy roots, seedlings, and cell suspension cultures (Fu, Zhang, Jin, et al., 2021; Ravazzolo et al., 2022; Tahmasebi et al., 2019). Here, we found that the EpMYC2-EpMYB2 module induces the MeJA signal on chicoric acid biosynthesis. When JAs are present, EpMYC2 is released. It activates the expression of EpMYB2, which further activates the expression of both primary and specialized chicoric acid

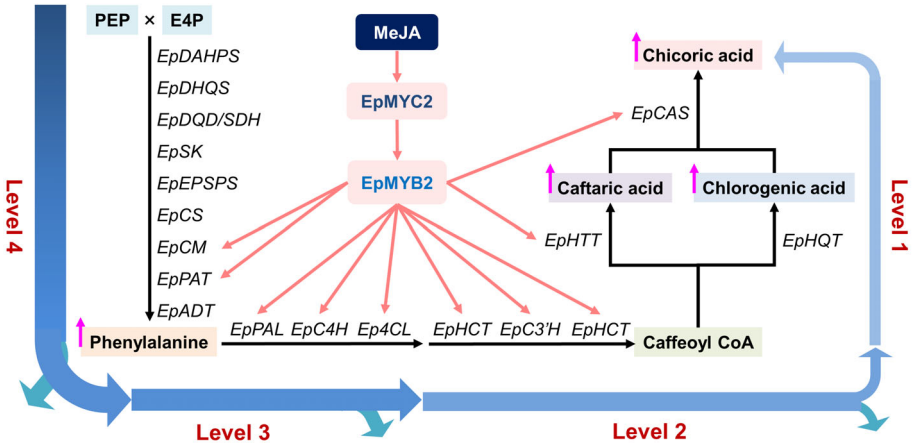

Figure 7. EpMYB2 positively regulates chicoric acid biosynthesis by activating both primary and specialized metabolic genes.
The chicoric acid biosynthetic pathway can be divided into four levels covering primary and secondary metabolism. The level 1 is the chicoric acid-specific pathway from caffeoyl CoA to chicoric acid. The level 2 is from *p*-coumaroyl CoA to caffeoyl CoA, sharing with other hydroxycinnamic acid derivatives. The level 3 is the common phenylpropanoid metabolic pathway from phenylalanine to *p*-coumaroyl CoA, sharing with other phenylpropanoids. The level 4 is from the shikimate pathway to aromatic amino acids biosynthesis, sharing with tryptophan and tyrosine. EpMYB2 positively regulates chicoric acid biosynthesis by activating both primary and specialized metabolic genes. Furthermore, it is activated by EpMYC2, a master regulator of the JA signaling pathway. The EpMYC2-EpMYB2 module is involved in the MeJA-induced chicoric acid biosynthesis.

biosynthetic genes and results in the biosynthesis of chicoric acid. This EpMYC2-EpMYB2 module explains the underlying mechanism of MeJA-induced chicoric acid biosynthesis and links the gap between environmental stress and metabolite biosynthesis (Figure 7). Due to the complex of JA responsive TFs (Afrin et al., 2015; Kazan & Manners, 2012; Ma et al., 2022), the interactions between EpJAZs and EpMYC2/EpMYB2 need further investigation.

In summary, we identified a MYB TF, EpMYB2, that positively regulates chicoric acid biosynthesis in purple coneflower by directly activating the expression of both primary and specialized metabolic genes covering primary and secondary metabolism. The identification of the EpMYC2-EpMYB2 module also links the gap between the JA signaling pathway and chicoric acid biosynthesis. These results further explain chicoric acid biosynthesis and pave the way to engineer chicoric acid production. Besides, compared to almost no chicoric acid production in the CK group, the considerable chicoric acid level of *EpMYB2* over-expression purple coneflower calli makes it be regarded as a raw material for the extraction of chicoric acid.

EXPERIMENTAL PROCEDURES

Plant materials and stress treatment

Purple coneflower seeds (PI 656830) were purchased from the U.S. National Plant Germplasm System. Sterile seedings were germinated as described previously (Fu, Zhang, Jin, et al., 2021). Two-month-old purple coneflower and one-month-old *N. benthamiana* were cultivated in a greenhouse (25°C, 16 h light/8 h dark, illumination intensity is 250 μmol m^{-2} sec^{-1}).

The purple coneflower transgenic callus was constructed as previously described with some modifications (Wang & To, 2004). CK and *2x35S: EpMYB2* vector were constructed using the GoldenBraid 2.0 method (Sarrion-Perdigones et al., 2013). The lower surface of purple coneflower leaf explants co-cultured with *Agrobacterium tumefaciens* strain LBA4404 was placed upward in E8 liquid medium containing MS salts (PhytoTechnology Laboratories, M524 and M533, Lenexa, KS, USA), 2% sucrose, 0.5 mg/L 6-benylaminopurine, 0.5 mg/L α-naphthaleneacetic acid, 100 mg/L kanamycin and 200 mg/L timentin. The leaf explants were placed in Tissue Culture Plate 24 well with 500 μL E8 liquid medium in each well and then incubated at 25°C in a growth chamber with a photoperiod of 16 h light (7000 lux) and 8 h dark. After 3–4 weeks, the surviving callus (with EGFP fluorescence) was cut away from explants at the edges and placed on an E8 solid medium (7 g/L phytagar). The callus was collected 3 months after the LBA4404 infection.

The cold treatment group was treated at 4°C in the dark for 6 h. The UV-B (ultraviolet-B) treatment group was treated at 25°C under 90 μW cm^{-2} UV-B for 6 h. NaCl and MeJA (methyl jasmonate) treatment groups were treated with 200 mM NaCl and 100 μM MeJA for 6 h, respectively. After treatment, calli were collected immediately for measurement. The CK group was collected at the beginning of the stress treatment. The purple coneflower root was treated with 100 μM MeJA for 24 h. After the treatment, the root was washed, separated, and collected from the whole plant.

Screening and analysis of chicoric acid biosynthesis regulators

The previously established multi-tissue transcriptome dataset of purple coneflower was used to screen potential chicoric acid biosynthesis regulators (Jin et al., 2024). The structural genes of the chicoric acid biosynthetic pathway were identified by BLASTP using our previously identified enzymes including EpHCT, EpHTT, EpHQT, and EpCAS. The upstream genes were identified by BLASTP using homologs in other species (Table S1). Hierarchical clustering of the biosynthetic genes was performed using Multiple Experiment Viewer (v4.9) with the following settings: single linkage method with Pearson correlation. The rest followed the initial

settings. Genes with an averaged TPM of each tissue of flowering purple coneflower <1 were excluded for co-expression analysis. *EpPAL*, *EpC4H*, *Ep4CL*, *EpC3′H*, *EpHTT*, and *EpCAS* were used as baits to screen chicoric acid biosynthesis regulators using CORREL functions from Microsoft EXCEL software ($r > 0.8$). The intersection of the six bait's co-expressed genes was used for further analysis (Supplemental Data Set S1).

After multiple sequence alignments by the ClustalW algorithm in MEGA X software (Thompson et al., 1994), phylogenetic analysis was performed in MEGA X software with a neighbor-joining statistical method, bootstrap method with 1000 bootstrap replications, and Jones-Taylor-Thornton model.

RNA isolation, RNA-seq and RT-qPCR analysis

All samples were ground into a fine powder within liquid nitrogen. Total RNA was isolated from each sample using FastPure® Plant Total RNA Isolation Kit (Vazyme, Nanjing, China) according to the manufacturer's instructions. The cDNA was generated from 1 μg of total RNA using PrimeScript™ RT reagent Kit with gDNA Eraser (Takara, Kuatscu, Japan).

The total RNA of CK and *EpMYB2*-OE calli were extracted, and the transcriptome was constructed and sequenced by the DNBSEQ platform (BGI, China). After sequencing, raw reads (containing joints containing more than 5% of the unknown base N, low quality) were filtered by SOAPnuke v1.4.0 software. The remaining clean reads were *de novo* assembled by Trinity v2.0.6 software, and transcripts were clustered by CD-HIT 4.6 to eliminate redundancy and obtain Unigenes.

RT–qPCR reaction systems and data analysis were performed as reported with some modifications (Ying et al., 2020). RT–qPCR was performed using a Bio-Rad CFX384 and iTaq Universal One-Step RT–qPCR Kits (Bio-Rad, Hercules, CA, USA) according to the manufacturer's instructions. RT–qPCR data were analyzed using *Eptubulin* as the reference gene. The relative expression of genes was calculated using the ΔCt method. The primers for RT–qPCR were shown in Supplemental Data Set S2.

Transient over-expression and subcellular localization in tobacco leaves

Candidate TFs were constructed into plasmid pEAQ-HT-DEST1 (Sainsbury et al., 2009) using the Gateway system and transformed into *A. tumefaciens* strain GV3101 by electroporation. The positive single colony was identified by PCR and grown in 400 μL LB liquid medium containing 50 mg/L kanamycin, 20 mg/L rifampicin, and 50 mg/L gentamicin for 24 h at 28°C with shaking at 180 rpm. The cultures (200 μL) were transferred to 10 mL of the same LB liquid medium and grown for 9 h to an OD_{600} value of 0.5–1. The *A. tumefaciens* culture was centrifuged at 4000 × ***g*** for 5 min, and resuspended the injection buffer (10 mM $MgCl_2$, 10 mM MES, 200 μM acetosyringone, pH5.6) to OD_{600} of 0.5. *A. tumefaciens* was activated at 28°C with shaking at 180 rpm for 1 h in the dark and injected into *N. benthamiana* leaves. Four days after injection, *N. benthamiana* leaves were harvested for measurement. For the subcellular localization experiment, *EpMYB2* without stop codon was cloned into the vector p35S1300EGFP to be fused with EGFP. The plants were grown in the dark for 24 h and prepared for microscopic observations. DAPI was injected into the leaves to label the nucleus 1 h before observation.

Determination of total phenolic content

The harvested samples were freeze-dried and then ground into fine powder. Total phenolic content was measured using the previous method (Fu et al., 2014). Briefly, dry powder (4–10 mg) was mixed with 100 times 70% methanol (0.4–1 mL) and extracted by ultrasound for 5 min at 4°C. After centrifugation, the supernatant was diluted with 70% methanol ten times. A liquid of 100 μL of diluted samples or gallic acid solutions (10–100 ng/mL, as a calibration standard) or ddH_2O (as blank) was mixed with 50 μL Folin–Ciocalteu's phenol reagent (Solarbio, Beijing, China), 50 μL sodium carbonate solution (20%, w/v) and 600 μL ddH_2O. After 40 min, 200 μL of the mixture was added to a 96-well colorless transparent plate to detect A_{765} by a microplate reader. Total phenolic content was expressed in mg gallic acid (GA) per 1 g dry powder.

Non-targeted metabolomics

Two pieces of calli were pooled as one biological replicate, and three replicates were used for metabolomic analysis. The samples were freeze-dried and ground into fine powder. The dry powder (4–10 mg) was mixed with 100 times methanol (0.4–1 mL) and extracted by ultrasound with 50% AMPL at 4°C, for 15 sec on 15 sec off, and a total of 10 min (Qsonica 700, Newton, CT, USA), the supernatant was collected for non-targeted metabolomics according to the previous method (Fu, Zhang, Deng, et al., 2021). Briefly, the data was acquired using a liquid chromatography-high-resolution mass spectrum (LC-HRMS) system (Nexera UHPLC LC-30A and AB SCIEX qTOF X500R). LC conditions were as follows: column, Hypersil Gold C18 (100 × 2.1 mm, 1.9 μm; Thermo Fisher Scientific, Waltham, MA, USA); column temperature, 40°C; flow rate, 0.4 mL/min; mobile phases, 0.1% formic acid (A) and acetonitrile (B); the gradient, 0–0.5 min 2% B, 0.5–6 min 2–20% B, 6–10 min 20–95% B, 10–12 min 95% B, 12–12.1 min 95–2% B, and 12.1–15 min 2% B; injection volume, 1.0 μL. MS conditions were as follows: information-dependent acquisition (IDA) model; electrospray ionization (ESI) source in negative polarity; ion source gas 1, 50 psi; ion source gas 2, 50 psi; curtain gas, 35 psi; CAD gas, 7; temperature, 450°C; spray voltage, −4500 V; for TOF-MS, the mass range, 100–1000 Da; declustering potential (DP), −80 V; DP spread, 0; collision energy (CE), −10 V; CE spread, 0; accumulation time, 0.1 sec; IDA criteria, small molecule; for TOF-MS/MS, the mass range, 50–1000 Da; DP, −80 V; DP spread, 0; CE, −40 V; CE spread, 20 V; accumulation time, 0.05 sec. A non-targeted screening workflow of SCIEX OS software (v1.7) was adopted with a medium peak detection sensitivity to export peak area for statistical analysis. The SIMCA software (v13.0, Umea, Sweden) was used for metabolomic analysis.

Cloning and binding site analysis of promoters

Promoters were cloned by the modified high-efficiency thermal asymmetric interlaced PCR (mhiTAIL-PCR) (Tan et al., 2019). Briefly, the pre-amplification has three steps: 10 high-stringency cycles for amplification of target single strands, 1 low-stringency cycle for binding of modified long arbitrary degenerate binding on single strands and priming, and 25 high-stringency cycles for amplification of target products. In the primary TAIL-PCR using, long specific products are preferentially amplified, whereas the non-specific products from the genome and the short specific products are less amplified by the TAIL-PCR and suppression-PCR. The second TAIL-PCR was performed to further amplify the specific products using inner primers. The fragment was ligated to the pEASY®-Blunt Simple Cloning Vector via the pEASY®-Blunt Simple Cloning Kit (TransGen Biotech, Beijing, China) and sequenced. The used primers were listed in Supplemental Data Set S2.

Promoter binding sites were analyzed by sequence alignment with binding sites MYB12BS (AtMYB12 binding site, CACCTACC,

TACCTAMC, and TAGCWACC) from previous studies (Zhang et al., 2015).

Dual-luciferase reporter assay

TFs were constructed into plasmid pEAQ-HT-DEST1 and used as the experimental group, while plasmid pEAQ-HT was used as the control group. The promoter was constructed into plasmid pGreenII0800. *A. tumefaciens* GV3101 carrying plasmids of the pEAQ series was mixed with *A. tumefaciens* GV3101 carrying plasmids of the pGreenII0800 series at a ratio of 10:1 (v/v) and injected into the leaves of *N. benthamiana*. Three days later, enzymatic activities of firefly luciferase (LUC) and renilla luciferase (REN) in *N. benthamiana* leaves were detected using the Dual-Luciferase Reporter Assay Kit (Vazyme, Nangjing, China).

Y1H assay

The Y1H assay was carried out using the Y1HGold-pAbAi Yeast One-Hybrid interaction proving kit (Coolaber, Beijing, China). A 100-bp promoter fragment containing the original or mutated MYB12BS or G-box site was constructed into a pAbAi vector. The pAbAi vector was linearized by the endonuclease *BstB*I and transformed into the yeast genome of the Y1HGold strain. The transformants were cultured on the SD medium without uracil (SD/-Ura) at 28°C for 2 days. The monoclonal colony was selected and identified by PCR and cultured on SD/-Ura with aureobasidin A (AbA, 0, 100, 200, 300, 500, 700, and 1000 ng/mL) for autoactivation analysis. The TF was cloned into the pGADT7 vector and transformed into the Y1HGold-pAbAi strain, and then cultured on the SD medium without leucine and with specific AbA concentration (SD/−Leu/+AbA) at 28°C for 3 days to test the interactions. The primers were listed in Supplemental Data Set S2.

Statistics analysis

Unless mentioned otherwise, all experiments in this paper were repeated at least three times, and results from representative datasets are presented. Data are expressed as mean ± SD (n = 3 or 4) and tested statistically significant difference ($^*P < 0.05$) between CK and the other group by unpaired Student's t-test. Statistically significant differences ($^*P < 0.05$) among groups were tested by one-way ANOVA following Tukey's multiple comparisons tests. The tests were conducted using GraphPad Prism 8 software.

ACCESSION NUMBERS

Sequence data from this article can be found in the GenBase in National Genomics Data Center, China National Center for Bioinformation / Beijing Institute of Genomics, Chinese Academy of Sciences, under the following accession numbers: *proEpMYB2* (C_AA049633.1), *proEpPAL* (C_AA001324.1), *proEpC4H* (C_AA001316.1), *proEp4CL* (C_AA001313.1), *proEpHCT* (C_AA001321.1), *proEpC3'H* (C_AA001315.1), *proEpHQT* (C_AA001322.1), *proEpHTT* (C_AA001323.1), *proEpCAS* (C_AA001317.1), *EpC3'H* (C_AA001303.1), *EpMYB2* (C_AA001310.1), *EpMYC2* (C_AA049630.1), *EpDAHPS* (C_AA049626.1), *EpDHQS* (C_AA049628.1), *EpDQD/SDH* (C_AA049627.1), *EpSK* (C_AA049632.1), *EpEPSPS* (C_AA049629.1), *EpCS* (C_AA049625.1), *EpCM* (C_AA049624.1), *EpPAT* (C_AA049631.1), and *EpADT* (C_AA049623.1) that are publicly accessible at https://ngdc.cncb.ac.cn/genbase.

ACKNOWLEDGMENTS

This work was financially supported by National Key Research and Development Program of China (No. 2023YFC3503903), National Natural Science Foundations of China (No. 31800258), Fundamental research funds for the central universities (SCU2023D003), and Natural Science Foundation of Sichuan Province, China (2023NSFSC1991).

AUTHOR CONTRIBUTIONS

GJ: Methodology, investigation, Resources, Data Curation, Writing – Original Draft, Writing – Review & Editing. ZD: Methodology, investigation. HW: Methodology, investigation, Writing – Review & Editing. YZ: Project administration, Conceptualization, Writing – Review & Editing. RF: Conceptualization, Methodology, investigation, Resources, Data Curation, Writing – Original Draft, Writing – Review & Editing, Visualization, Project administration, Funding acquisition.

CONFLICT OF INTEREST

The authors declare no conflict of interest.

DATA AVAILABILITY STATEMENT

The raw transcriptome sequence data of flowering purple coneflower tissues (GSA: CRA009264) and purple coneflower calli (GSA: CRA013312) reported in this paper have been deposited in the Genome Sequence Archive in National Genomics Data Center, China National Center for Bioinformation/-Beijing Institute of Genomics, Chinese Academy of Sciences that are publicly accessible at https://ngdc.cncb.ac.cn/gsa.

SUPPORTING INFORMATION

Additional Supporting Information may be found in the online version of this article.

Figure S1. RT–qPCR confirms chicoric acid biosynthetic gene expression patterns from RNA-seq.

Figure S2. Candidate chicoric acid biosynthesis regulator is identified by co-expression and phylogenetic analysis.

Figure S3. EpMYB2 is an R2R3-MYB.

Figure S4. Construction and identification of positive transgenic purple coneflower calli.

Figure S5. The regulation of flavonoid biosynthesis by EpMYB2.

Figure S6. Scatter plots of differentially expressed genes for CK and *EpMYB2*-OE purple coneflower calli.

Figure S7. EpMYB2 activates *proEpPAL* by targeting the MYB12BS site.

Figure S8. MYC2 is conserved in purple coneflower.

Figure S9. EpMYC2 directly binds to the −126 bp G-box of *proEpMYB2* determined by Y1H.

Table S1. BLAST baits for the identification of biosynthetic genes.

Data Set S1. Transcription factors co-expressed with chicoric acid biosynthetic genes.

Data Set S2. Primer sequences were used in this study.

REFERENCES

Afrin, S., Huang, J.-J. & Luo, Z.-Y. (2015) JA-mediated transcriptional regulation of secondary metabolism in medicinal plants. *Science Bulletin*, **60**, 1062–1072.

Burlou-Nagy, C., **Banica, F.**, **Jurca, T.**, **Vicas, L.G.**, **Marian, E.**, **Muresan, M.E.** ***et al.*** (2022) *Echinacea purpurea* (L.) Moench: biological and pharmacological properties-a review. *Plants-Basel*, **11**, 1244.

Creelman, R.A., **Tierney, M.L.** & **Mullet, J.E.** (1992) Jasmonic acid/methyl jasmonate accumulate in wounded soybean hypocotyls and modulate wound gene expression. *Proceedings of the National Academy of Sciences of the United States of America*, **89**, 4938–4941.

Czemmel, S., **Stracke, R.**, **Weisshaar, B.**, **Cordon, N.**, **Harris, N.N.**, **Walker, A.R.** ***et al.*** (2009) The grapevine R2R3-MYB transcription factor VvMYBF1 regulates Flavonol synthesis in developing grape berries. *Plant Physiology*, **151**, 1513–1530.

De Geyter, N., **Gholami, A.**, **Goormachtig, S.** & **Goossens, A.** (2012) Transcriptional machineries in jasmonate-elicited plant secondary metabolism. *Trends in Plant Science*, **17**, 349–359.

Deng, Y. & **Lu, S.** (2017) Biosynthesis and regulation of phenylpropanoids in plants. *Critical Reviews in Plant Sciences*, **36**, 257–290.

Dong, N.Q. & **Lin, H.X.** (2021) Contribution of phenylpropanoid metabolism to plant development and plant-environment interactions. *Journal of Integrative Plant Biology*, **63**, 180–209.

Erb, M. & **Kliebenstein, D.J.** (2020) Plant secondary metabolites as defenses, regulators, and primary metabolites: the blurred functional trichotomy. *Plant Physiology*, **184**, 39–52.

Fu, R., **Li, J.**, **Yu, H.**, **Zhang, Y.**, **Xu, Z.** & **Martin, C.** (2021) The Yin and Yang of traditional Chinese and Western medicine. *Medicinal Research Reviews*, **41**, 3182–3200.

Fu, R., **Zhang, P.**, **Deng, Z.**, **Jin, G.**, **Guo, Y.** & **Zhang, Y.** (2021) Diversity of antioxidant ingredients among *Echinacea* species. *Industrial Crops and Products*, **170**, 113699.

Fu, R., **Zhang, P.**, **Jin, G.**, **Wang, L.**, **Qi, S.**, **Cao, Y.** ***et al.*** (2021) Versatility in acyltransferase activity completes chicoric acid biosynthesis in purple coneflower. *Nature Communications*, **12**, 1563.

Fu, R., **Zhang, P.**, **Jin, G.**, **Wei, S.**, **Chen, J.**, **Pei, J.** ***et al.*** (2022) Substrate promiscuity of acyltransferases contributes to the diversity of hydroxycinnamic acid derivatives in purple coneflower. *The Plant Journal*, **110**, 802–813.

Fu, R., **Zhang, Y.**, **Guo, Y.**, **Liu, F.** & **Chen, F.** (2014) Determination of phenolic contents and antioxidant activities of extracts of *Jatropha curcas* L. seed shell, a by-product, a new source of natural antioxidant. *Industrial Crops and Products*, **58**, 265–270.

Guo, Q., **Major, I.T.** & **Howe, G.A.** (2018) Resolution of growth–defense conflict: mechanistic insights from jasmonate signaling. *Current Opinion in Plant Biology*, **44**, 72–81.

Hong, B., **Grzech, D.**, **Caputi, L.**, **Sonawane, P.**, **Lopez, C.E.R.**, **Kamileen, M.O.** ***et al.*** (2022) Biosynthesis of strychnine. *Nature*, **607**, 617–622.

Isah, T., **Umar, S.**, **Mujib, A.**, **Sharma, M.P.**, **Rajasekharan, P.E.**, **Zafar, N.** ***et al.*** (2018) Secondary metabolism of pharmaceuticals in the plant in vitro cultures: strategies, approaches, and limitations to achieving higher yield. *Plant Cell, Tissue and Organ Culture*, **132**, 239–265.

Jiang, C.K. & **Rao, G.Y.** (2020) Insights into the diversification and evolution of R2R3-MYB transcription factors in plants. *Plant Physiology*, **183**, 637–655.

Jin, G., **Deng, Z.**, **Wang, H.**, **Li, W.**, **Su, L.**, **Zhang, Y.** ***et al.*** (2024) A stress-responsive R2R3-MYB transcription factor, EpMYB1 is involved in the regulation of anthocyanin biosynthesis in purple coneflower. *Industrial Crops and Products*, **209**, 118043.

Karsch-Volk, M., **Barrett, B.** & **Linde, K.** (2015) Echinacea for preventing and treating the common cold. *JAMA*, **313**, 618–619.

Kazan, K. & **Manners, J.M.** (2012) JAZ repressors and the orchestration of phytohormone crosstalk. *Trends in Plant Science*, **17**, 22–31.

Kindscher, K. (2016) *Echinacea*. Springer Nature. https://doi.org/10.1007/978-3-319-18156-1

Li, B., **Fan, R.**, **Guo, S.**, **Wang, P.**, **Zhu, X.**, **Fan, Y.** ***et al.*** (2019) The Arabidopsis MYB transcription factor, MYB111 modulates salt responses by regulating flavonoid biosynthesis. *Environmental and Experimental Botany*, **166**, 103807.

Li, Y., **Chen, M.**, **Wang, S.**, **Ning, J.**, **Ding, X.** & **Chu, Z.** (2015) AtMYB11 regulates caffeoylquinic acid and flavonol synthesis in tomato and tobacco. *Plant Cell, Tissue and Organ Culture*, **122**, 309–319.

Li, Y., **Chen, Y.**, **Zhou, L.**, **You, S.**, **Deng, H.**, **Chen, Y.** ***et al.*** (2020) MicroTom metabolic network: rewiring tomato metabolic regulatory network throughout the growth cycle. *Molecular Plant*, **13**, 1203–1218.

Liu, C., **Long, J.**, **Zhu, K.**, **Liu, L.**, **Yang, W.**, **Zhang, H.** ***et al.*** (2016) Characterization of a citrus R2R3-MYB transcription factor that regulates the Flavonol and hydroxycinnamic acid biosynthesis. *Scientific Reports*, **6**, 25352.

Liu, C.-Z., **Abbasi, B.H.**, **Gao, M.**, **Murch, S.J.** & **Saxena, P.K.** (2006) Caffeic acid derivatives production by hairy root cultures of *Echinacea purpurea*. *Journal of Agricultural and Food Chemistry*, **54**, 8456–8460.

Liu, J., **Osbourn, A.** & **Ma, P.** (2015) MYB transcription factors as regulators of phenylpropanoid metabolism in plants. *Molecular Plant*, **8**, 689–708.

Liu, Y., **Du, M.**, **Deng, L.**, **Shen, J.**, **Fang, M.**, **Chen, Q.** ***et al.*** (2019) MYC2 regulates the termination of jasmonate signaling via an autoregulatory negative feedback loop. *Plant Cell*, **31**, 106–127.

Lou, S.L., **Guo, X.**, **Liu, L.**, **Song, Y.**, **Zhang, L.**, **Jiang, Y.Z.** ***et al.*** (2022) Allelic shift in cis-elements of the transcription factor RAP2.12 underlies adaptation associated with humidity in *Arabidopsis thaliana*. *Science Advances*, **8**, eabn8281.

Luo, J., **Butelli, E.**, **Hill, L.**, **Parr, A.**, **Niggeweg, R.**, **Bailey, P.** ***et al.*** (2008) AtMYB12 regulates caffeoyl quinic acid and flavonol synthesis in tomato: expression in fruit results in very high levels of both types of polyphenol. *The Plant Journal*, **56**, 316–326.

Ma, P., **Pei, T.**, **Lv, B.**, **Wang, M.**, **Dong, J.** & **Liang, Z.** (2022) Functional pleiotropism, diversity, and redundancy of salvia miltiorrhiza Bunge JAZ family proteins in jasmonate-induced tanshinone and phenolic acid biosynthesis. *Horticulture Research*, **9**, uhac166.

Matsui, K., **Oshima, Y.**, **Mitsuda, N.**, **Sakamoto, S.**, **Nishiba, Y.**, **Walker, A.R.** ***et al.*** (2018) Buckwheat R2R3 MYB transcription factor FeMYBF1 regulates flavonol biosynthesis. *Plant Science*, **274**, 466–475.

Nakatsuka, T., **Saito, M.**, **Yamada, E.**, **Fujita, K.**, **Kakizaki, Y.** & **Nishihara, M.** (2012) Isolation and characterization of GtMYBP3 and GtMYBP4, orthologues of R2R3-MYB transcription factors that regulate early flavonoid biosynthesis, in gentian flowers. *Journal of Experimental Botany*, **63**, 6505–6517.

Newman, D.J. & **Cragg, G.M.** (2020) Natural products as sources of new drugs over the nearly four decades from 01/1981 to 09/2019. *Journal of Natural Products*, **83**, 770–803.

Prouse, M.B. & **Campbell, M.M.** (2012) The interaction between MYB proteins and their target DNA binding sites. *Biochimica et Biophysica Acta*, **1819**, 67–77.

Pyvovarenko, T. & **Lopato, S.** (2011) Isolation of plant transcription factors using a yeast one-hybrid system. *Methods in molecular biology (Clifton, N.J.)*, **754**, 45–66.

Ramezannezhad, R., **Aghdasi, M.** & **Fatemi, M.** (2019) Enhanced production of cichoric acid in cell suspension culture of *Echinacea purpurea* by silver nanoparticle elicitation. *Plant Cell, Tissue and Organ Culture*, **139**, 261–273.

Ravazzolo, L., **Ruperti, B.**, **Frigo, M.**, **Bertaiola, O.**, **Pressi, G.**, **Malagoli, M.** ***et al.*** (2022) C3H expression is crucial for methyl Jasmonate induction of Chicoric acid production by *Echinacea purpurea* (L.) Moench cell suspension cultures. *International Journal of Molecular Sciences*, **23**, 11179.

Reed, J., **Orme, A.**, **El-Demerdash, A.**, **Owen, C.**, **Martin, L.B.B.**, **Misra, R.C.** ***et al.*** (2023) Elucidation of the pathway for biosynthesis of saponin adjuvants from the soapbark tree. *Science*, **379**, 1252–1264.

Ren, S., **Yuan, Y.**, **Wang, H.** & **Zhang, Y.** (2022) G2-LIKE CAROTENOID REGULATOR (SlGCR) is a positive regulator of lutein biosynthesis in tomato. *aBIOTECH*, **3**, 267–280.

Sainsbury, F., **Thuenemann, E.C.** & **Lomonossoff, G.P.** (2009) pEAQ: versatile expression vectors for easy and quick transient expression of heterologous proteins in plants. *Plant Biotechnology Journal*, **7**, 682–693.

Sarrion-Perdigones, A., **Vazquez-Vilar, M.**, **Palaci, J.**, **Castelijns, B.**, **Forment, J.**, **Ziarsolo, P.** ***et al.*** (2013) GoldenBraid 2.0: a comprehensive DNA assembly framework for plant synthetic biology. *Plant Physiology*, **162**, 1618–1631.

Serin, E.A.R., **Nijveen, H.**, **Hilhorst, H.W.M.** & **Ligterink, W.** (2016) Learning from co-expression networks: possibilities and challenges. *Frontiers in Plant Science*, **7**, 444.

Shah, S.A., **Sander, S.**, **White, C.M.**, **Rinaldi, M.** & **Coleman, C.I.** (2007) Evaluation of echinacea for the prevention and treatment of the common cold: a meta-analysis. *Lancet Infectious Diseases*, **7**, 473–480.

Shen, Q., **Lu, X.**, **Yan, T.**, **Fu, X.**, **Lv, Z.**, **Zhang, F.** ***et al.*** (2016) The jasmonate-responsive AaMYC2 transcription factor positively regulates artemisinin biosynthesis in *Artemisia annua*. *The New Phytologist*, **210**, 1269–1281.

Smith, T., **Resetar, H.** & **Mortonc, C.** (2022) US sales of herbal supplements increase by 9.7% in 2021. *HerbalGram*, **136**, 42–69.

Song, C., **Cao, Y.**, **Dai, J.**, **Li, G.**, **Manzoor, M.A.**, **Chen, C.** ***et al.*** (2022) The multifaceted roles of MYC2 in plants: toward transcriptional reprogramming and stress tolerance by Jasmonate signaling. *Frontiers in Plant Science*, **13**, 868874.

Tabar, R.S., **Moieni, A.** & **Monfared, S.R.** (2019) Improving biomass and chicoric acid content in hairy roots of *Echinacea purpurea* L. *Biologia (Bratisl.)*, **74**, 941–951.

Tahmasebi, A., **Ebrahimie, E.**, **Pakniyat, H.**, **Ebrahimi, M.** & **Mohammadi-Dehcheshmeh, M.** (2019) Insights from the *Echinacea purpurea* (L.) Moench transcriptome: global reprogramming of gene expression patterns towards activation of secondary metabolism pathways. *Industrial Crops and Products*, **132**, 365–376.

Tan, J., **Gong, Q.**, **Yu, S.**, **Hou, Y.**, **Zeng, D.**, **Zhu, Q.** ***et al.*** (2019) A modified high-efficiency thermal asymmetric interlaced PCR method for amplifying long unknown flanking sequences. *Journal of Genetics and Genomics*, **46**, 363–366.

Thompson, J.D., **Higgins, D.G.** & **Gibson, T.J.** (1994) CLUSTAL W: improving the sensitivity of progressive multiple sequence alignment through sequence weighting, position-specific gap penalties and weight matrix choice. *Nucleic Acids Research*, **22**, 4673–4680.

Vogt, T. (2010) Phenylpropanoid biosynthesis. *Molecular Plant*, **3**, 2–20.

Wang, F., **Kong, W.**, **Wong, G.**, **Fu, L.**, **Peng, R.**, **Li, Z.** ***et al.*** (2016) AtMYB12 regulates flavonoids accumulation and abiotic stress tolerance in transgenic Arabidopsis thaliana. *Molecular Genetics and Genomics*, **291**, 1545–1559.

Wang, H.-M. & **To, K.-Y.** (2004) Agrobacterium-mediated transformation in the high-value medicinal plant *Echinacea purpurea*. *Plant Science*, **166**, 1087–1096.

Wu, Y., **Wen, J.**, **Xia, Y.**, **Zhang, L.** & **Du, H.** (2022) Evolution and functional diversification of R2R3-MYB transcription factors in plants. *Horticulture Research*, **9**, uhac058.

Xiang, Y., **Zhang, Y.** & **Fu, R.** (2022) Chicoric acid biosynthesis during seed germination provides purple coneflower with better allelochemical. *Industrial Crops and Products*, **177**, 114572.

Yang, C.Q., **Fang, X.**, **Wu, X.M.**, **Mao, Y.B.**, **Wang, L.J.** & **Chen, X.Y.** (2012) Transcriptional regulation of plant secondary metabolism. *Journal of Integrative Plant Biology*, **54**, 703–712.

Yang, M., **Wu, C.**, **Zhang, T.**, **Shi, L.**, **Li, J.**, **Liang, H.** ***et al.*** (2022) Chicoric acid: natural occurrence, chemical synthesis, biosynthesis, and their bioactive effects. *Frontiers in Chemistry*, **10**, 888673.

Ying, S., **Su, M.**, **Wu, Y.**, **Zhou, L.**, **Fu, R.**, **Li, Y.** ***et al.*** (2020) Trichome regulator SlMIXTA-like directly manipulates primary metabolism in tomato fruit. *Plant Biotechnology Journal*, **18**, 354–363.

Yuan, Y., **Ren, S.**, **Liu, X.**, **Su, L.**, **Wu, Y.**, **Zhang, W.** ***et al.*** (2022) SlWRKY35 positively regulates carotenoid biosynthesis by activating the MEP pathway in tomato fruit. *New Phytologist*, **234**, 164–178.

Zhai, Q., **Deng, L.** & **Li, C.** (2020) Mediator subunit MED25: at the nexus of jasmonate signaling. *Current Opinion in Plant Biology*, **57**, 78–86.

Zhang, Y., **Butelli, E.**, **Alseekh, S.**, **Tohge, T.**, **Rallapalli, G.**, **Luo, J.** ***et al.*** (2015) Multi-level engineering facilitates the production of phenylpropanoid compounds in tomato. *Nature Communications*, **6**, 8635.

Zheng, H., **Fu, X.**, **Shao, J.**, **Tang, Y.**, **Yu, M.**, **Li, L.** ***et al.*** (2023) Transcriptional regulatory network of high-value active ingredients in medicinal plants. *Trends in Plant Science*, **28**, 856.

Zhou, M. & **Memelink, J.** (2016) Jasmonate-responsive transcription factors regulating plant secondary metabolism. *Biotechnology Advances*, **34**, 441–449.